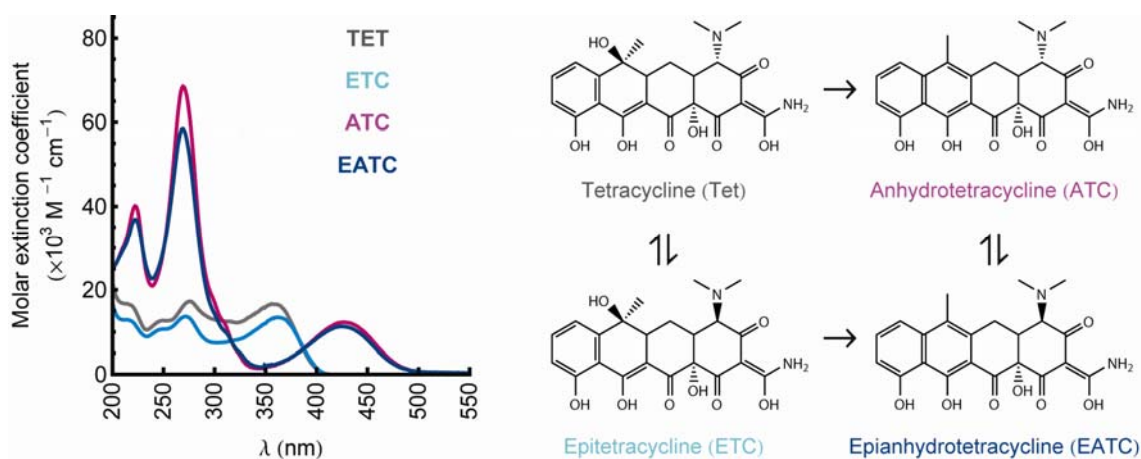


Supplementary Material for

Chemical decay of an antibiotic inverts selection for resistance

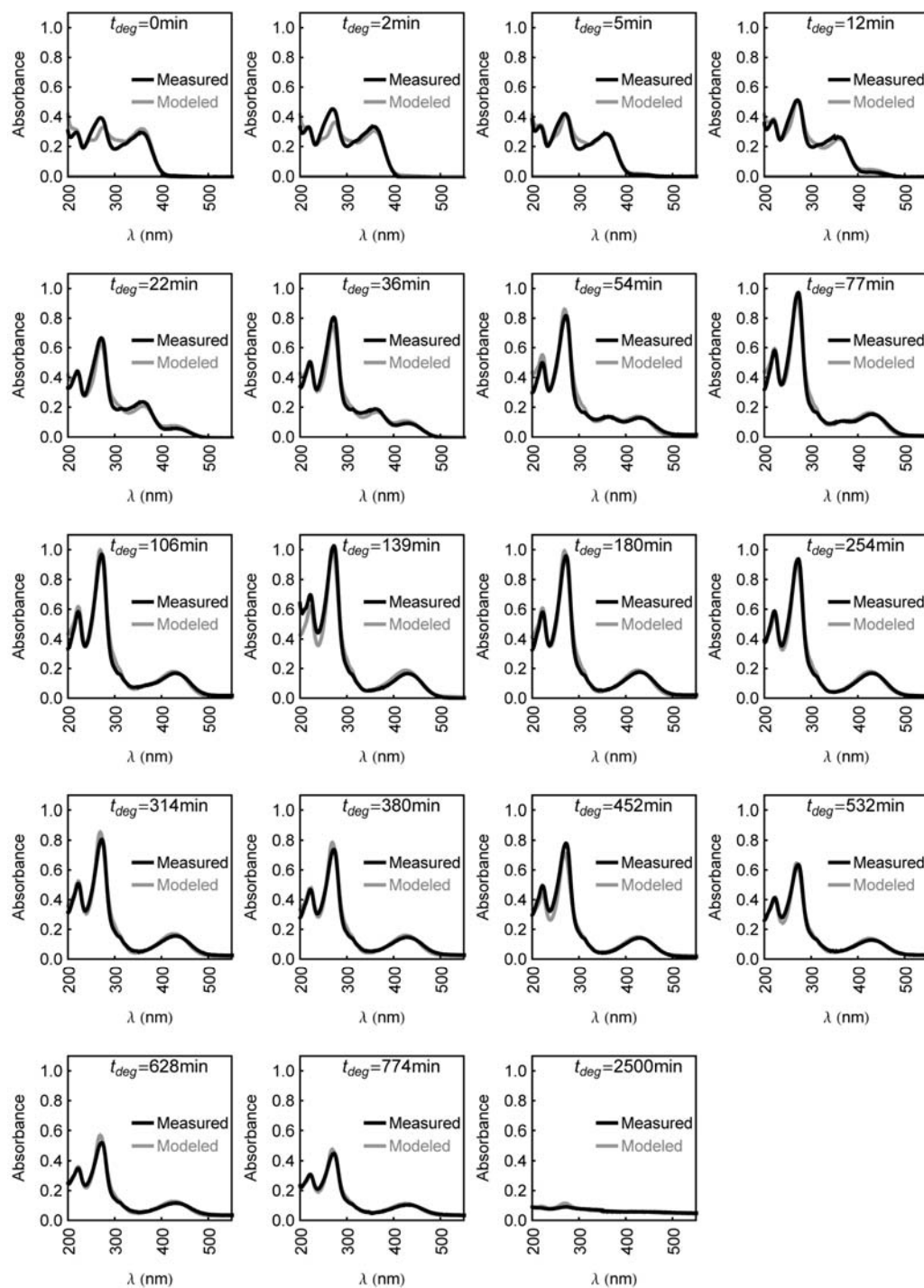
Adam C. Palmer, Elaine Angelino and Roy Kishony.

Supplementary Figures



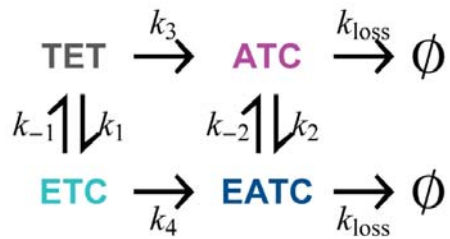
Supplementary Figure 1. Absorbance spectra and structures of tetracycline

and its degradation products. Absorbance spectra measured in aqueous solution, at $10 \mu\text{g/mL}$, of tetracycline (Tet; gray), epitetracycline (ETC; cyan), anhydrotetracycline (ATC; magenta) and epianhydrotetracycline (EATC; dark blue).



Supplementary Figure 2. Measured and modeled spectra of degraded tetracycline solutions. Measured spectra of tetracycline solutions exposed to degrading conditions for different lengths of time (black), aligned with modeled spectra (gray). Modeled spectra are calculated as a linear combination of the spectra of individual compounds (Supplementary Fig. 1), with coefficients given by the kinetic model of tetracycline decay (Supplementary Fig. 3), which describes the proportion

of each compound as a function of time in degrading conditions (see Fig. 1c). After very prolonged degradation ($t_{deg} = 2500$ min) the spectrum is flat but non-zero, and so the linear combination of spectra also contains a term for the $t_{deg} = 2500$ min spectrum, with coefficient given by the proportion of further degradation products, i.e. following further decay of ATC and EATC (denoted “ \emptyset ” in the kinetic model; Supplementary Fig. 3). The parameter k_{loss} is fitted to minimize the sum of square errors between these measured and modeled spectra. To maximize distinction between the similar spectra of epimers, errors were only summed over the most characteristic absorption peaks, located at the wavelength ranges 250-290nm and 325-400nm.



$$\frac{d[\text{Tet}]}{dt} = k_{-1} \times [\text{ETC}] - (k_1 + k_3) \times [\text{Tet}]$$

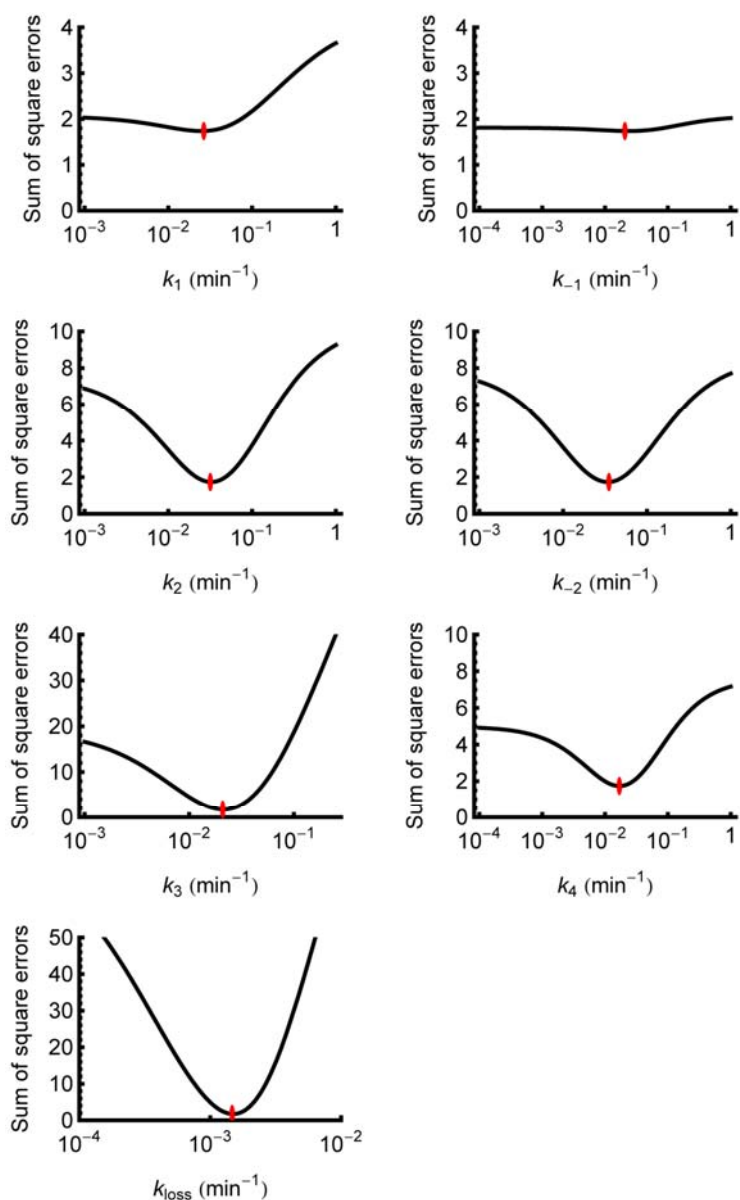
$$\frac{d[\text{ETC}]}{dt} = k_1 \times [\text{Tet}] - (k_{-1} + k_4) \times [\text{ETC}]$$

$$\frac{d[\text{ATC}]}{dt} = k_3 \times [\text{Tet}] + k_{-2} \times [\text{EATC}] - (k_2 + k_{\text{loss}}) \times [\text{ATC}]$$

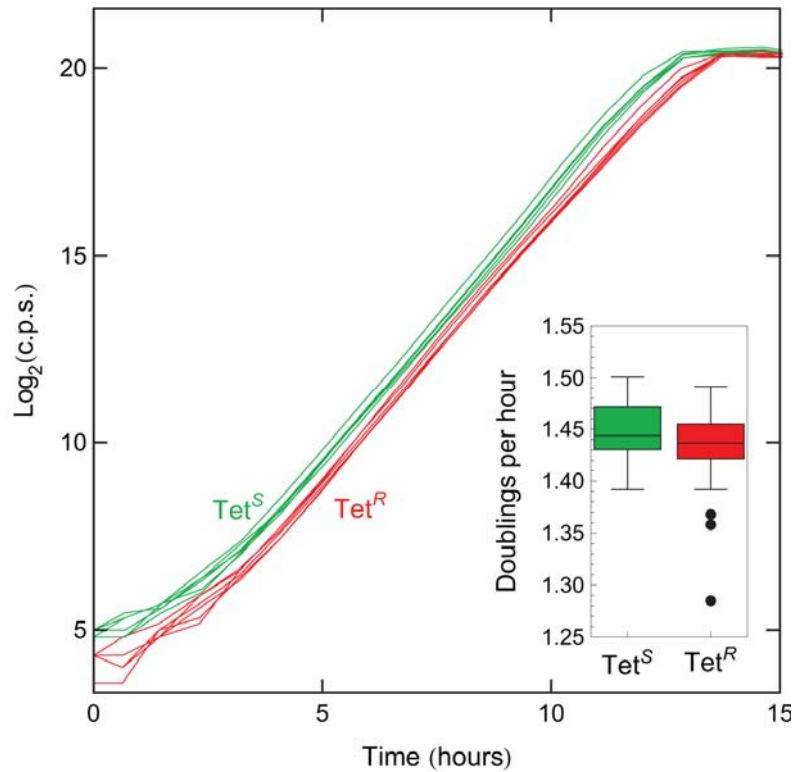
$$\frac{d[\text{EATC}]}{dt} = k_4 \times [\text{ETC}] + k_2 \times [\text{ATC}] - (k_{-2} + k_{\text{loss}}) \times [\text{EATC}]$$

$$\frac{d[\emptyset]}{dt} = k_{\text{loss}} \times ([\text{ATC}] + [\text{EATC}])$$

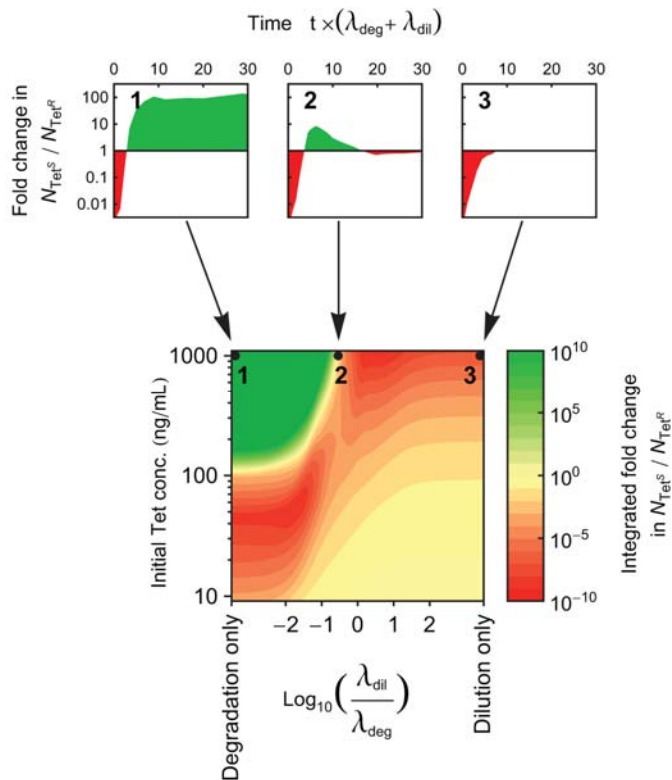
Supplementary Figure 3. Kinetic model of tetracycline decay. Reaction scheme for the kinetic model of tetracycline decay constructed by Yuen and Sokoloski¹, extended to account for the slow loss of degradation products at very long timescales (k_{loss}). The shaded areas in Figure 1c are constructed from this model, utilizing values of k_1 , k_{-1} , k_2 , k_{-2} , k_3 and k_4 which were experimentally determined by Yuen and Sokoloski¹, and a fitted value of k_{loss} (Supplementary Table 1).



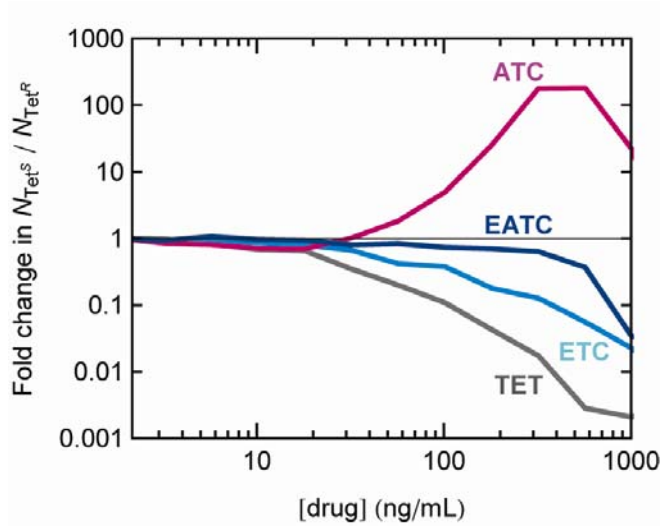
Supplementary Figure 4. Parameter sensitivity of the kinetic model of tetracycline decay. Plotting the error between measured and modeled spectra of degraded tetracycline solutions (Supplementary Fig. 2) demonstrates the consistency of the rate constants measured by Yuen and Sokolosi¹ with this study. Note that only the characteristic wavelength ranges 250-290nm and 325-400nm were utilized. The parameter values used in the kinetic model (Supplementary Table 1) are marked in red. k_{loss} was absent from the kinetic model of Yuen and Sokolosi¹, and so was fitted to minimize the sum of square errors.



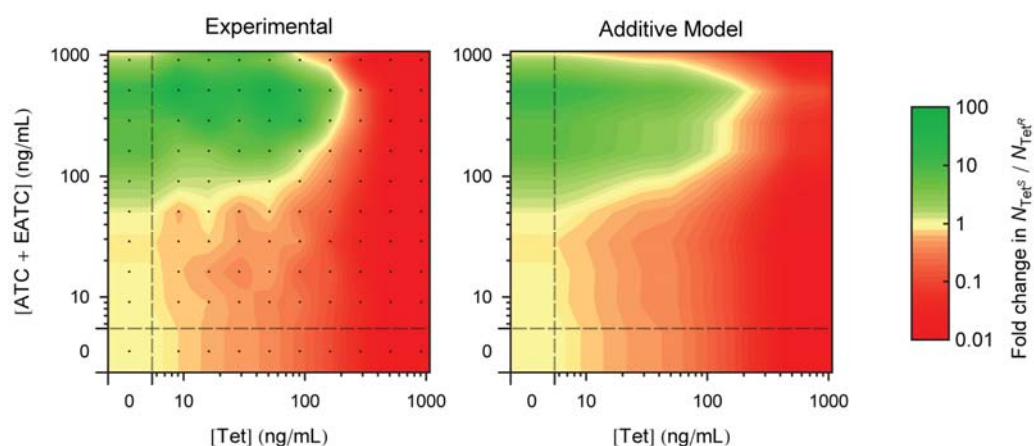
Supplementary Figure 5. Tet^S and Tet^R strains have equal growth rates in the absence of tetracycline. Growth rates were measured with high resolution over the course of 15 doublings using bioluminescence based measurements of cell density^{2,3} (Methods). Six representative growth curves each are presented for the Tet^S (green) and Tet^R (red) strains. Inset: Boxplot of growth rate measurements of the Tet^S and Tet^R strains (n=36 each).



Supplementary Figure 6. Net selection for/against tetracycline resistance depends upon both the means of drug loss and the initial drug concentration. For any given initial drug concentration and rates of dilution and degradation (λ_{dil} and λ_{deg} , respectively), a linear trajectory is defined across the surface of Figure 2c, describing how selective pressure changes over time as the drug and its degradation products are lost from the environment: examples are trajectories 1, 2, and 3 from Figures 2c and 2d. Integrating $\log(N_{Tet}^S / N_{Tet}^R)$ along a trajectory provides the net selective pressure resulting from a given initial drug concentration and ratio of dilution and degradation rates, $\lambda_{dil} / \lambda_{deg}$. On the left edge of the plot drug loss is by degradation only, with the dilution rate increasing in relative magnitude towards the right; on the right edge drug loss is by dilution only. Trajectory 1 illustrates a timecourse of selection resulting in net selection against resistance. Trajectory 2 illustrates neutral net selection, where periods of selection for and against resistance cancel out over time. Trajectory 3 illustrates net selection for resistance.



Supplementary Figure 7. Tetracycline and its degradation products each have a different impact on selection for resistance. Selective pressures of Tet and individual degradation products ETC, ATC, and EATC, measured by competition between Tet^S and Tet^R strains (see Fig. 2a).



Supplementary Figure 8. Combinations of tetracycline and its degradation products produce selective pressures which are well predicted by Bliss additivity. Selective pressure for (red) or against (green) resistance across a drug gradient of Tet and a 1:1 mixture of ATC and EATC; on the left experimentally measured (as per Fig. 2a) and on the right ('Additive Model') calculated from the effects along the axes of the 'Experimental' panel, assuming additive drug interactions, i.e. by summing the changes in $\log(N_{Tet}^S / N_{Tet}^R)$.

Methods

Strains and Media

Fluorescently labeled strains MC4100-YFP and MC4100-CFP, described previously⁵, were transformed with plasmid pBT107-6A to create a Tet resistant strain, or with the parent plasmid pACYC177 to create a Tet sensitive strain. pBT107-6A carries the Tn10 tetracycline resistance determinant, with a *tetA* promoter down-mutation which has been demonstrated to provide higher fitness in the presence of 10 $\mu\text{g}\cdot\text{mL}^{-1}$ Tet than either stronger or weaker promoters^{6,7}.

All fitness measurements were performed in M63 minimal medium (2 $\text{g}\cdot\text{L}^{-1}$ $(\text{NH}_4)_2\text{SO}_4$, 13.6 $\text{g}\cdot\text{L}^{-1}$ KH_2PO_4 , 0.5 $\text{mg}\cdot\text{L}^{-1}$ $\text{FeSO}_4\cdot 7\text{H}_2\text{O}$) supplemented with 0.2% glucose, 0.01% casamino acids, 1mM MgSO_4 and 1.5 μM thiamine, and also 100 $\mu\text{g}\cdot\text{mL}^{-1}$ ampicillin and 50 $\mu\text{g}\cdot\text{mL}^{-1}$ kanamycin for the maintenance of pACYC177 based plasmids. Drug solutions were made from powder stocks (Sigma, Vetranal analytical standard: tetracycline hydrochloride, catalog no. 3174; epitetracycline hydrochloride, catalog #37918; anhydrotetracycline hydrochloride, catalog #37919; epianhydrotetracycline hydrochloride, catalog #37921) dissolved in ethanol, with drug gradients made by serial dilution in M63 medium.

Tetracycline degradation

Powdered tetracycline was dissolved in 1M phosphoric acid, pH 1.5, at 400 $\mu\text{g}/\text{mL}$. Aliquots were incubated at 75°C and transferred to ice at various time points. These frozen samples were diluted 40 \times into M63 media for fitness assay, or into water for spectroscopy.

Spectroscopy and determination of chemical composition from spectra

All spectra were recorded at 10 $\mu\text{g}/\text{mL}$ in aqueous solution, on a Cary 300 spectrophotometer (Varian). The kinetic model of Yuen and Sokoloski¹, modified to include a reaction for the slow further decay of Tet degradation products with rate constant k_{loss} , successfully fitted the time series of spectra (Supplementary Figs. 2,

3) using all other rate constants as previously measured by HPLC¹. Allowing all rate constants to be simultaneously fitted to all spectra produces only a 2% reduction in the sum of square errors; the previously measured parameters have values that minimize errors in the spectral alignment, for all parameters for which a well defined minimum exists (Supplementary Fig. 4, Supplementary Table 1). Species concentrations were estimated from spectra at individual timepoints (points in Figure 1c) by numerically searching for the local minimum in alignment error over the characteristic wavelength ranges 250-290nm and 325-400nm, starting from the composition predicted by the kinetic model; numerical minimization was performed by the FindMinimum function of *Mathematica 7.0* (Wolfram).

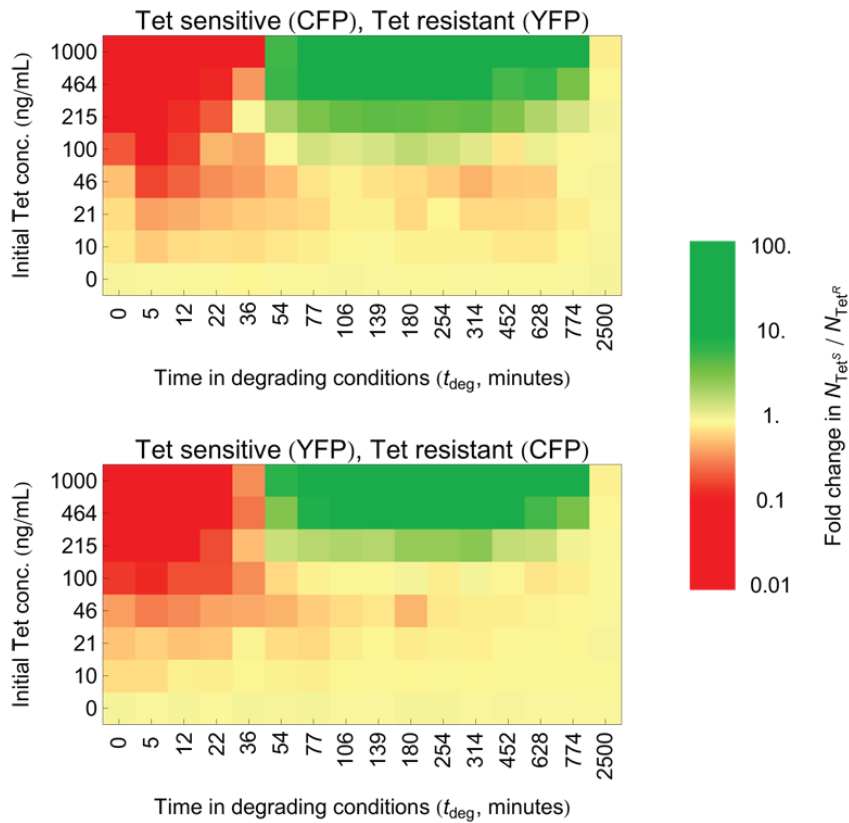
Competitive fitness assay

Selection between resistant and sensitive cells by a particular chemical environment was measured by mixing stationary phase cultures of resistant and sensitive strains at 1:1 ratio, and further diluting 1:100 into fresh media containing the chemical environment of interest. Competitive growth occurred throughout 24 hours of growth with shaking at 30°C in clear, flat bottomed 96-well plates (Corning #3595), sealed with adhesive lids (Perkin Elmer #6005185). Sensitive and resistant cells were differentially labeled with a chromosomally integrated YFP or CFP gene driven by the P_{lac} promoter, which is constitutive in the *lacI* strains used here. To obtain stronger fluorescence signals, the stationary phase cultures obtained after 24 hours of competition were subcultured 1:100 into fresh drug-free media, and grown as before for between 90 and 180 minutes, before the ratio of yellow to cyan fluorescent cells was counted by flow cytometry (Becton Dickinson LSRII; CFP excited at 405nm, emission detected through 505LP and 525/550nm filters; YFP excited at 488nm, emission also detected through 505LP and 525/550nm filters). Plating and colony counting of selected wells confirmed that the final subculturing and brief growth did not alter the ratio N_{Tet^S} / N_{Tet^R} , within the margin of error of counting 200 - 500 colonies per plate. The selective pressures presented in Figure 2c and Supplementary Figure 7 are the average of two experiments, one where fluorescent labels were swapped between Tet^S and Tet^R strains. No substantial difference was detected between dye-swaps, indicating that the use of differential dyes does not

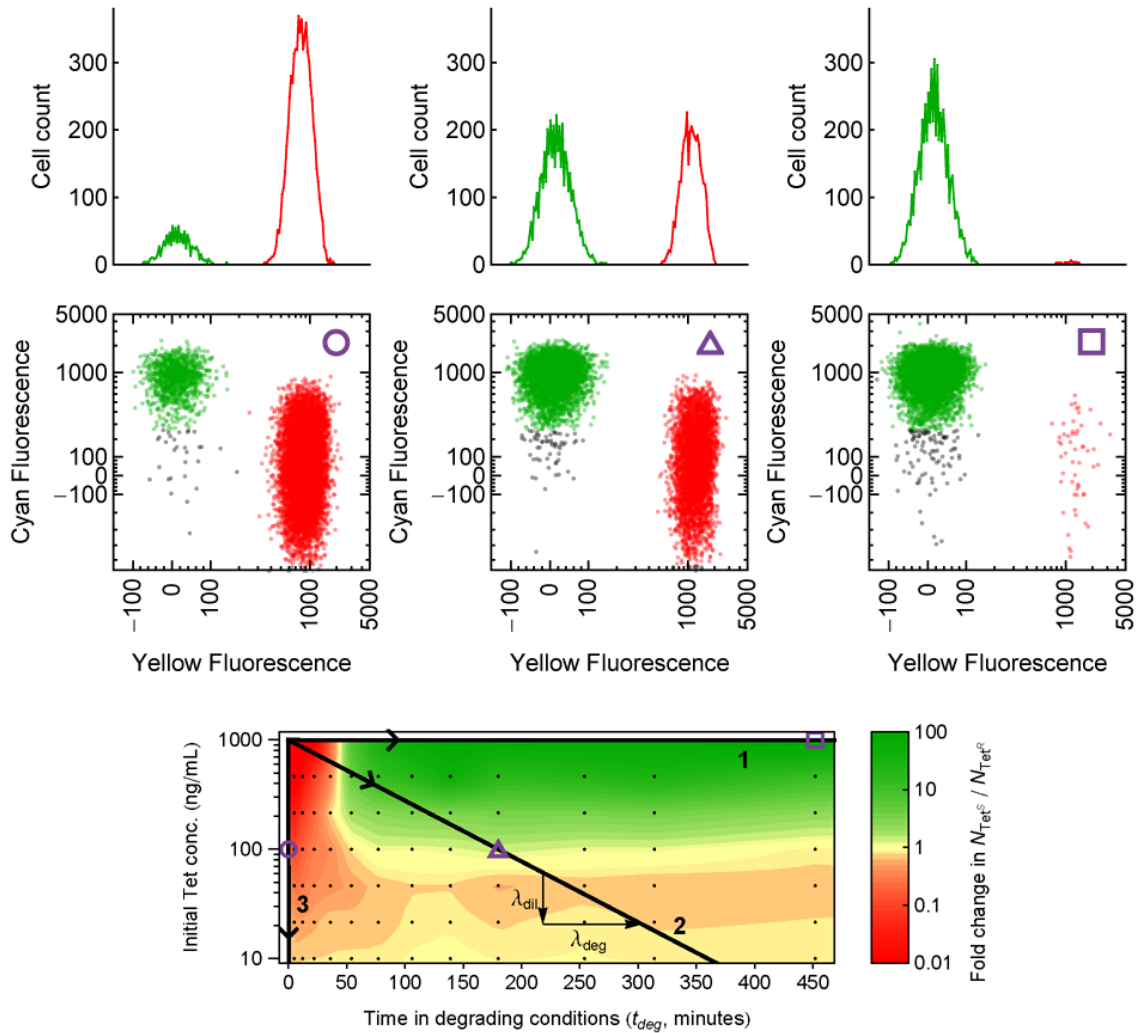
influence $N_{\text{Tet}^{\text{S}}} / N_{\text{Tet}^{\text{R}}}$ ratio (Supplementary Fig. 9). At least 16 wells per plate were drug-free, for precise measurement of $N_{\text{Tet}^{\text{S}}} / N_{\text{Tet}^{\text{R}}}$ ratio in non-selective conditions. The mean ratio $N_{\text{Tet}^{\text{S}}} / N_{\text{Tet}^{\text{R}}}$ (mean determined on log scale) in these drug-free wells provided the reference point, determined separately for each plate, for the fold change in $N_{\text{Tet}^{\text{S}}} / N_{\text{Tet}^{\text{R}}}$. Sample flow cytometry data from three points in Figure 2c are presented in Supplementary Figure 10, demonstrating selection for, against, and neutral with respect to resistance.

Growth rate assay

Tet^S and Tet^R strains were transformed with a plasmid-borne, constitutively expressed bacterial bioluminescence operon². Photon counting of growing bioluminescent cultures allows precise measurements of cell densities over many orders of magnitudes (e.g. Supplementary Fig. 5). Cultures were grown in black 96-well plates (Corning #3792) sealed with clear adhesive lids (Perkin Elmer #6005185). Readings were made by a Perkin Elmer TopCount NXT Microplate Scintillation and Luminescence Counter, stored in a 30°C room at 70% humidity, with duplicate 1 second readings per well. Wells contained 100µL of media inoculated with approximately 10 to 100 cells from fresh -80°C frozen cultures. Growth rate is the slope of the logarithm of photon counts per second (c.p.s.), and is taken from the line of best fit spanning the fastest 5 doublings.



Supplementary Figure 9. Different permutations of fluorescent labels do not influence selection for/against resistance by tetracycline degradation products. Selective pressure for (red) or against resistance (green) by Tet and its degradation products (Fig. 2c) was measured by averaging the results of two competition experiments: between Tet^S-CFP and Tet^R-YFP; and between Tet^S-YFP and Tet^R-CFP. Here these measurements are presented separately, where it can be seen that competition between Tet^S and Tet^R strains is not influenced by the permutation of fluorescent labels.



Supplementary Figure 10. Measurement of selection for/against resistance by flow cytometry. Flow cytometry measurements of N_{Tet^S} and N_{Tet^R} , for representative data points in Figure 2c (reproduced here with selected data points marked in purple). These scatter plots of raw measurements of cyan and yellow fluorescence are presented in ‘logicle’ scale to prevent distortion of low signals by logarithmic scaling⁴. These points demonstrate selection for resistance (circle), no selection (triangle), and selection against resistance (square). Above the cyan-yellow scatter plots are histograms summing the number of resistant cells (red; N_{Tet^R}) and sensitive cells (green; N_{Tet^S}).

Parameter	Value (min ⁻¹)	Source	ΔE (%)
k_1	0.0265	Ref. 1	0.04
k_{-1}	0.0207	Ref. 1	0.04
k_2	0.0317	Ref. 1	0.06
k_{-2}	0.0352	Ref. 1	0.08
k_3	0.0209	Ref. 1	0.09
k_4	0.0169	Ref. 1	0.001
k_{loss}	0.00147	fitted*	N/A*

Supplementary Table 1. Parameter values of the kinetic model of tetracycline decay. The consistency of parameters measured in Ref. 1 with this study's spectra of degraded tetracycline solutions (Supplementary Fig. 2) can be quantitated by the error in the alignment between measured and modeled spectra. Specifically, we define the error E as

$$E = \sum_{t_{deg}} \int (A_{\lambda}^{measured} - A_{\lambda}^{modelled})^2 d\lambda$$

where λ is integrated over the ranges 250-290nm and 325-400nm. E can be evaluated with modeled spectra produced either by the parameters in Ref. 1, or by parameters which are fitted to minimize E . For each single parameter then, we determine $\Delta E = E(\text{Ref. 1 parameter}) / E(\text{best fit parameter}) - 1$, which describes how close the parameters in Ref. 1 are to minimizing E . We see that they are indeed extremely close to minimizing the alignment error (see also Supplementary Fig. 4). When all parameters are simultaneously fitted, $\Delta E = 2\%$. Values taken from Ref. 1 are averages of duplicate measurements at 75°C. Note that although Tet and ATC exert the strongest selective effects (Supplementary Fig. 7), the kinetic model cannot be accurately simplified to these two compounds alone. The equilibrium constant for epimerization between Tet and ETC ($k_1/k_{-1} = 1.3$) is different from the equilibrium constant between ATC and EATC ($k_2/k_{-2} = 0.90$). Consequently, even after epimerization reactions have reached equilibrium, the dehydration reaction does not bring about a net 1:1 conversion between Tet and ATC.

References

1. Yuen, P.H. & Sokoloski, T.D. *J Pharm Sci* **66**, 1648--1650 (1977).
2. Kishony, R. & Leibler, S. *J Biol* **2**, 14 (2003).
3. Yeh, P., Tschumi, A.I. & Kishony, R. *Nat Genet* **38**, 489--494 (2006).
4. Parks, D.R., Roederer, M. & Moore, W.A. *Cytometry A* **69**, 541-51 (2006).
5. Hegreness, M., Shores, N., Hartl, D. & Kishony, R. *Science* **311**, 1615--1617 (2006).
6. Daniels, D.W. & Bertrand, K.P. *J Mol Biol* **184**, 599--610 (1985).
7. Lenski, R.E. et al. *Mol Ecol* **3**, 127--135 (1994).